


 Cite this: *Chem. Commun.*, 2024, 60, 582

 Received 20th October 2023,  
 Accepted 5th December 2023

DOI: 10.1039/d3cc05142k

rsc.li/chemcomm

# Enantioselective synthesis of 3-(*N*-indolyl)quinolines containing axial and central chiralities†

 Ken Yamanomoto,<sup>ab</sup> Kota Yamamoto,<sup>a</sup> Satoshi Yoshida,<sup>c</sup> Sota Sato<sup>ib,cd</sup> and Takahiko Akiyama<sup>ib,\*a</sup>

Quinoline and indole are important core structures in biologically active compounds and materials. Atropisomeric biaryls consisting of quinoline and indole are a unique class of axially chiral molecules. We report herein enantioselective synthesis of 3-(*N*-indolyl)quinolines having both C–N axial chirality and carbon central chirality by a photoredox Minisci-type addition reaction catalyzed by a chiral lithium phosphate/Ir-photoredox complex. The catalytic system enabled access to a unique class of 3-(*N*-indolyl)quinolines with high chemo-, regio-, and stereoselectivities in good yields through the appropriate choice of an acid catalyst and a photocatalyst. This is the first example of the synthesis of 3-(*N*-indolyl)quinoline atropisomers in a highly enantioselective manner.

Axial chirality is an important structural motif in organic chemistry. Axially chiral bis(hetero)arenes have recently shown potential use in a wide range of fields<sup>1–3</sup> including materials science,<sup>4</sup> medicinal chemistry,<sup>5</sup> and catalyst design.<sup>6</sup> A range of efficient synthetic methods have been reported lately.<sup>7</sup> In contrast to the general procedure for installing one chiral element, the procedure for the simultaneous construction of multiple chiral elements, particularly elements having multiple chiralities such as axial and central chiralities, remains underdeveloped.<sup>8</sup> The development of novel catalytic methodology for the stereoselective synthesis of heterobiaryls possessing carbon central chirality continues to be a formidable task.

Quinolines with axial chirality and central chirality are an important class of compounds in pharmaceuticals and biologically active compounds,<sup>5b,9</sup> and the catalyst-controlled synthesis of chiral quinolines has attracted significant attention over the last decade.<sup>7,10</sup> For instance, a quinoline-based biaryl HIV integrase inhibitor showed high potential, and the balance between potency and metabolic stability is tuned by the functional groups on C3 and C4 positions of quinoline.<sup>11–13</sup> Despite expectations placed on axially chiral 3-arylquinolines and their analogues as a key structure in chemistry, their applications are rare because the reported synthetic routes are limited. To the best of our knowledge, the only example of the synthesis of enantio-enriched axially chiral 3-arylquinolines is the recent work of Gustafson and co-workers on the dynamic kinetic resolution of 2-fluoro-3-arylquinolines by the  $S_NAr$  reaction with thiophenol using chiral cinchona-urea catalyst, in which some limitations hindered the path to high enantioselectivity.<sup>13</sup> The enantioselective synthesis of quinolines with multiple chiral elements is a challenging task that remains unexplored.

As part of our continued interest in developing atroposelective reactions using chiral phosphoric acid (CPA) catalysis<sup>14</sup> and for addressing the above-mentioned issues, we envisaged that the Minisci-type radical functionalization by photoredox-chiral acid hybrid catalysis would provide the desired quinolines in high yields and with excellent enantioselectivities.<sup>15</sup> The stereoselective Minisci reaction under photoredox catalysis is a powerful method for the transformation of heteroarenes under mild conditions. Phipps and co-workers disclosed an enantioselective Minisci-type addition reaction by Ir photocatalysis-CPA under visible-light irradiation (Scheme 1b).<sup>16</sup> In 2022, Xiao and co-workers applied the dual photoredox-CPA catalysis to the atroposelective synthesis of 5-arylbiopyrimidines containing axial and central chiralities (Scheme 1c).<sup>17</sup> However, the atroposelective Minisci reaction for the synthesis of quinolines bearing axial and carbon central chirality has not been reported, probably because of its inability to meet the high efficiency, regioselectivity, chemoselectivity, and stereoselectivity requirements.<sup>18</sup>

<sup>a</sup> Department of Chemistry, Faculty of Science, Gakushuin University, Mejiro, Toshima-ku, Tokyo 171-8588, Japan. E-mail: takahiko.akiyama@gakushuin.ac.jp

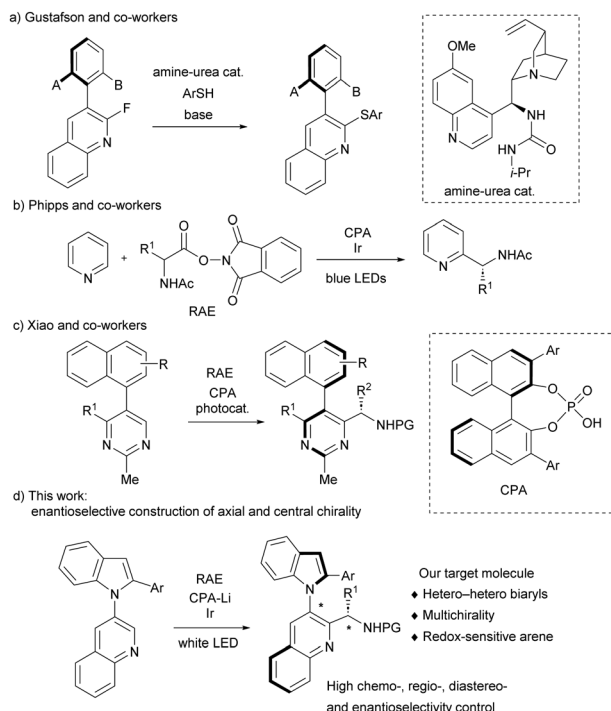
<sup>b</sup> Department of Chemistry, Faculty of Science, Tokyo University of Science, Kagurazaka, Shinjuku-ku, Tokyo 162-8601, Japan

<sup>c</sup> Department of Applied Chemistry, School of Engineering, The University of Tokyo, 7-3-1 Hongo, Bunkyo-ku, Tokyo 113-8656, Japan

<sup>d</sup> Division of Advanced Molecular Science, Institute for Molecular Science, National Institutes of Natural Sciences, 5-1 Higashiyama, Myodaiji-cho, Okazaki, Aichi 444-8787, Japan

† Electronic supplementary information (ESI) available. CCDC 2286593. For ESI and crystallographic data in CIF or other electronic format see DOI: <https://doi.org/10.1039/d3cc05142k>





**Scheme 1** (a) Atroposelective functionalization reaction of 3-arylquinoline. (b) Asymmetric Minisci reaction by CPA-Ir photocatalysis. (c) Asymmetric synthesis of 5-arylpyrimidines containing axial and central chiralities. (d) This study.

Our reaction design is described in Fig. 1d. Redox-active ester (RAE) derived from an amino acid was selected as a radical precursor in the Minisci-type radical addition reaction with achiral 3-aryl quinolines. We started our investigation by evaluating the catalytic activity of chiral BINOL-derived

phosphoric acid<sup>19</sup> and its metal salt<sup>20,21</sup> in the reaction of 3-(2'-phenyl-*N*-indolyl)quinoline **1a** with alanine-derived RAE **2a**. The desired reaction proceeded smoothly in the presence of 10 mol% of lithium phosphate derived from 3,3'-[2,4,6-(*i*-Pr)<sub>3</sub>C<sub>6</sub>H<sub>2</sub>]-substituted (*R*)-BINOL (**TRIP-Li**) and 2 mol% of Ir[(ppy)<sub>2</sub>(dtbbpy)]PF<sub>6</sub> at 60 °C in toluene to afford biaryl **3a** in 91% yield, with 20 : 1 dr, and 90% ee (Table 1, entry 1). The use of phosphoric acid (**TRIP**) gave **3a** with similar diastereoselectivity and enantioselectivity albeit in a lower yield (entry 2 vs. entry 1). The other metal phosphates examined were ineffective. Control experiments established that lithium phosphate, Ir photocatalyst, and light are essential for the alkylation of quinoline under these conditions (see ESI†). Further catalyst screening demonstrated that the use of bulky lithium phosphate (**4-Li**) improved the enantioselectivity of **3a** to 96% (entry 7). The combination of lithium phosphate and Ir[(ppy)<sub>2</sub>(dtbbpy)]PF<sub>6</sub> was crucial for achieving the excellent yield and high chemo-, regio-, and stereoselectivities (for detail, see ESI†, S1). The absolute stereochemistry of **3a** was unambiguously determined to be (*S,S*) by single-crystal X-ray diffraction analysis,<sup>22</sup> and those of other compounds were surmised by analogy.

With the optimized reaction conditions in hand, we explored the scope of our method by performing reactions of a range of 3-(*N*-indolyl)quinolines with several RAEs (Fig. 2). Quinolines bearing electron-donating and electron-withdrawing groups on indole participated in the reaction to afford the corresponding adducts in good yields and with excellent stereoselectivities. In addition to alanine-derived RAE **2a**, phenylalanine- and tyrosine-derived RAEs could also be used as radical precursors, and the corresponding adducts were obtained in high yields and with good to excellent stereoselectivities. We also explored the steric and electronic nature of the phenyl group at C2 position of indole. The desired

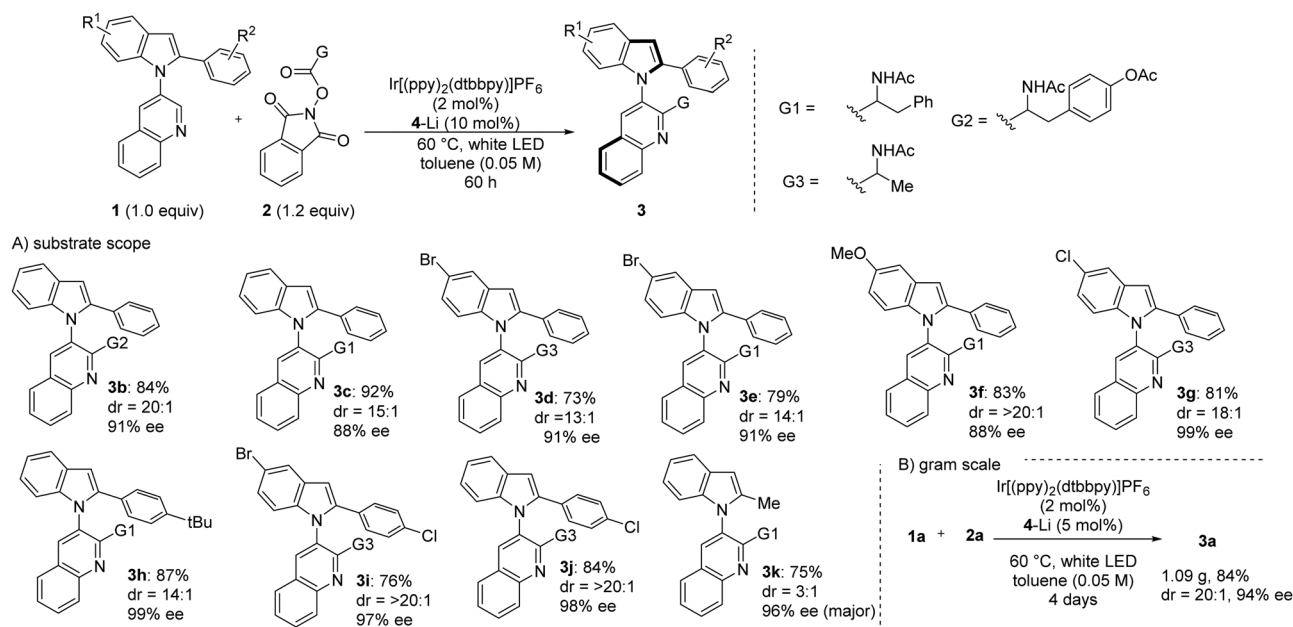


**Fig. 1** Asymmetric synthesis of 3-(*N*-indolyl)quinolines.



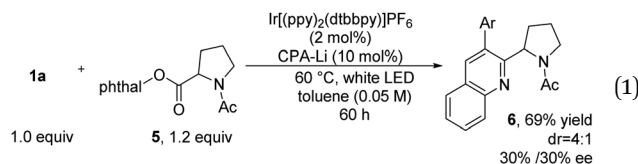
Table 1 Optimization of conditions for asymmetric Minisci reaction

Entry <sup>a</sup>	Deviation from standard conditions	Yield <sup>b</sup> (%)	dr <sup>c</sup>	ee <sup>d</sup> (%)
1	None	91	20:1	90
2	TRIP	42	20:1	87
3	TRIP-Na	< 10	—	—
4	TRIP-K	Trace	—	—
5	TRIP-Mg	21	12:1	20
6	TRIP-Ca	37	12:1	34
7	4-Li	92	20:1	96

<sup>a</sup> Reactions were performed using 0.05 mmol of **1a** and 0.06 mmol of **2a** in 0.5 mL of toluene in the presence of 2 mol% of Ir[(ppy)<sub>2</sub>(dtbbpy)]PF<sub>6</sub> and 10 mol% of acid. <sup>b</sup> Isolated yield. <sup>c</sup> Determined from crude NMR. <sup>d</sup> Determined by chiral HPLC analysis.

<sup>a</sup> Reactions were performed using 0.05 mmol of **1a** and 0.06 mmol of **2a** in 0.5 mL of toluene in the presence of 2 mol% of Ir[(ppy)<sub>2</sub>(dtbbpy)]PF<sub>6</sub> and 10 mol% of acid. <sup>b</sup> Isolated yield. <sup>c</sup> Determined from crude NMR. <sup>d</sup> Determined by chiral HPLC analysis.

**1a** with proline-derived RAE **5**, which contains no hydrogen bond donor under the optimized reaction conditions furnished the corresponding adduct **6** in a good yield albeit with low optical purity (eqn (1)). The N-H moiety in RAE was critical for the excellent enantioselectivity because it formed a hydrogen bond between the alkyl radical and the chiral phosphate. Photoluminescence quenching experiments verified the initial single-electron transfer step in this photoredox process (see ESI<sup>†</sup>). Strong quenching of the fluorescence of photoexcited Ir[(ppy)<sub>2</sub>(dtbbpy)]PF<sub>6</sub> was observed, suggesting that the excited Ir complex reduced RAE. The radical trapping experiment showed that TEMPO inhibited the formation of the desired product, and alkylated TEMPO was detected by HRMS (See ESI<sup>†</sup>). From these results and previous reports,<sup>16</sup> we propose a reaction mechanism, as shown in Fig. 2. The single-electron reduction of RAE by the photoexcited Ir(III) complex would generate alkyl radical **2'** along with oxidized Ir(IV) complex, which could be verified by the Stern–Volmer luminescence quenching experiments (see ESI<sup>†</sup>). The radical addition of **2'** to chiral acid-activated quinoline would afford cationic intermediate *intA*. The subsequent intramolecular proton transfer would furnish oxonium species *intB*. Oxidation of resulting intermediate *intB* would provide the alkylated quinoline and release the Lewis acid. We suppose that the transformation of *intA* into *intB* would be the rate-determining step, and the central chirality would be controlled in this step.<sup>23</sup>



In conclusion, we have developed a strategy for the enantioselective synthesis of 2-alkyl-3-(*N*-indolyl)quinolines bearing both axial and central chiralities by the combined use of chiral lithium phosphate and Ir photocatalyst. The reaction took place smoothly to give the addition products in high yields and with high to excellent optical purity under mild conditions and offered access to a variety of quinolines bearing both C–N axial chirality and central carbon chirality. This is the first report on the stereoselective synthesis of axially chiral *N*-indolylquinolines with high enantioselectivity. Further investigations to expand the utility of this methodology and its application to bioactive molecular synthesis are under way in our laboratory.

We thank Professor Yoshiyuki Inaguma (Gakushuin University) for cyclic voltammetry measurement, Professor Koichi Iwata (Gakushuin University) for emission spectra measurement. Financial support from JSPS (KAKENHI Grant Numbers JP20H00380 and JP23H01965 for T. A.) is appreciated. We thank KEK Photon Factory BL-17A (No. 2021G589) for the use of X-ray diffraction instruments and Spring-8 BL45XU (No. 2022B1320) for the preliminary diffraction examination.

## Conflicts of interest

There are no conflicts to declare.

Fig. 2 Proposed reaction mechanism.

reaction smoothly proceeded to give **3h**, **3i**, and **3j** in excellent yields and with excellent enantioselectivities. Replacing the 2-phenyl substituent with a methyl group gave corresponding product **3k** with low diastereoselectivity (dr = 3:1) but with excellent enantioselectivity (major diastereomer: 96% ee). In order to demonstrate the robustness and scalability of this method, enantio-enriched quinoline **3a** was synthesized on a gram scale (Fig. 1B). Even though the catalyst loading of **4-Li** was reduced to 5 mol%, the desired product was obtained without loss of stereoselectivity.

Experiments were performed to gain insight into the mechanism of this reaction. The Minisci reaction of 3-(*N*-indolyl)quinoline



## Notes and references

- 1 (a) B. Zilate, A. Castrogiovanni and C. Sparr, *ACS Catal.*, 2018, **8**, 2981; (b) Y. B. Wang and B. Tan, *Acc. Chem. Res.*, 2018, **51**, 534; (c) C. X. Liu, W. W. Zhang, S. Y. Yin, Q. Gu and S. L. You, *J. Am. Chem. Soc.*, 2021, **143**, 14025; (d) J. Wang, C. Zhao and J. Wang, *ACS Catal.*, 2021, **11**, 12520; (e) J. K. Cheng, S. H. Xiang, S. Li, L. Ye and B. Tan, *Chem. Rev.*, 2021, **121**, 4805; (f) H.-R. Sun, A. Sharif, J. Chen and L. Zhou, *Chem. – Eur. J.*, 2023, **29**, e202300183; (g) G.-J. Mei, W. L. Koay, C.-Y. Guan and Y. Lu, *Chem.*, 2022, **8**, 1855; (h) P. Rodriguez-Salamanca, R. Fernández, V. Hornillos and J. M. Lassaletta, *Chem. – Eur. J.*, 2022, **28**, e202104442.
- 2 (a) *Atropisomerism and Axial Chirality*, ed. J. M. Lassaletta, World Scientific, 2018; (b) *Axially Chiral Compounds: Asymmetric Synthesis and Applications*, ed. B. Tan, Wiley-VCH, Weinheim, 2021.
- 3 For recent papers on enantioselective synthesis of (hetero)-(hetero) biaryls, see: (a) G.-J. Mei, J. J. Wong, W. Zheng, A. A. Nangia, K. N. Houk and Y. Lu, *Chemistry*, 2021, **7**, 2743; (b) X.-M. Wang, P. Zhang, Q. Xu, C.-Q. Guo, D.-B. Zhang, C.-J. Lu and R.-R. Liu, *J. Am. Chem. Soc.*, 2021, **143**, 15005; (c) O. Kitagawa, *Acc. Chem. Res.*, 2021, **54**, 719; (d) H.-H. Zhang and F. Shi, *Acc. Chem. Res.*, 2022, **55**, 6829; (e) J. K. Cheng, S.-H. Xiang and B. Tan, *Acc. Chem. Res.*, 2022, **55**, 2920; (f) K. W. Chen, Z. H. Chen, S. Yang, S. F. Wu, Y. C. Zhang and F. Shi, *Angew. Chem., Int. Ed.*, 2022, **61**, e202116829; (g) X. Zhu, H. Wu, Y. Wang, G. Huang, F. Wang and X. Li, *Chem. Sci.*, 2023, **14**, 8564; (h) Z.-H. Chen, T.-Z. Li, N.-Y. Wang, X.-F. Ma, S.-F. Ni, Y.-C. Zhang and F. Shi, *Angew. Chem., Int. Ed.*, 2023, **62**, e202300419; (i) S.-Y. Yin, Q. Zhou, C.-X. Liu, Q. Gu and S.-L. You, *Angew. Chem., Int. Ed.*, 2023, **62**, e202305067.
- 4 C. Ge, W. Zhang, W. L. Tan, C. R. McNeill and X. Gao, *ACS Mater. Lett.*, 2022, **4**, 363.
- 5 (a) P. W. Glunz, *Bioorg. Med. Chem. Lett.*, 2018, **28**, 53; (b) S. R. LaPlante, L. D. Fader, K. R. Fandrick, D. R. Fandrick, O. Hucke, R. Kemper, S. P. F. Miller and P. J. Edwards, *J. Med. Chem.*, 2011, **54**, 7005; (c) K. T. Barrett, A. J. Metrano, P. R. Rablen and S. J. Miller, *Nature*, 2014, **509**, 71.
- 6 *Catalytic Asymmetric Synthesis*, ed. T. Akiyama and I. Ojima, John Wiley & Sons, Hoboken, 4th edn, 2022.
- 7 (a) T. Sun, Z. Zhang, Y. Su, H. Cao, Y. Zhou, G. Luo and Z.-C. Cao, *J. Am. Chem. Soc.*, 2023, **145**, 15721; (b) J. A. Carmona, P. Rodriguez-Salamanca, R. Fernández, J. M. Lassaletta and V. Hornillos, *Angew. Chem., Int. Ed.*, 2023, **62**, e202306981.
- 8 For examples of construction of axial and central chiralities, see: (a) J. Zhang, X. Huo, J. Xiao, L. Zhao, S. Ma and W. Zhang, *J. Am. Chem. Soc.*, 2021, **143**, 12622; (b) V. Hornillos, J. A. Carmona, A. Ros, J. Iglesias-Sigüenza, J. López-Serrano, R. Fernández and J. M. Lassaletta, *Angew. Chem., Int. Ed.*, 2018, **57**, 3777; (c) C. Ma, F.-T. Sheng, H.-Q. Wang, S. Deng, Y.-C. Zhang, Y. Jiao, W. Tan and F. Shi, *J. Am. Chem. Soc.*, 2020, **142**, 15686; (d) F. Wang, J. Jing, Y. Zhao, X. Zhu, X.-P. Zhang, L. Zhao, P. Hu, W.-Q. Deng and X. Li, *Angew. Chem., Int. Ed.*, 2021, **60**, 16628; (e) J. Wang, H. Chen, L. Kong, F. Wang, Y. Lan and X. Li, *ACS Catal.*, 2021, **11**, 9151.
- 9 A. F. Pozharskii, A. T. Soldatenkov and A. R. Katritzky, *Heterocycles in Life and Society: An Introduction to Heterocyclic Chemistry, Biochemistry and Applications*, Wiley-VCH, 2nd edn, 2011.
- 10 (a) J. Wang, M.-W. Chen, Y. Ji, S.-B. Hu and Y.-G. Zhou, *J. Am. Chem. Soc.*, 2016, **138**, 10413; (b) Y.-D. Shao, M.-M. Dong, Y.-A. Wang, P.-M. Cheng, T. Wang and D.-J. Cheng, *Org. Lett.*, 2019, **21**, 4831; (c) Q. Wang, Z.-J. Cai, C.-X. Liu, Q. Gu and S.-L. You, *J. Am. Chem. Soc.*, 2019, **141**, 9504; (d) A. Romero-Arenas, V. Hornillos, J. Iglesias-Sigüenza, R. Fernández, J. López-Serrano, A. Ros and J. M. Lassaletta, *J. Am. Chem. Soc.*, 2020, **142**, 2628; (e) A. B. Rolka, N. Archipowa, R. J. Kutta, B. König and F. D. Toste, *J. Org. Chem.*, 2023, **88**, 6509.
- 11 L. D. Fader, E. Malenfant, M. Parisien, R. Carson, F. Bilodeau, S. Landry, M. Pesant, C. Brochu, S. Morin, C. Chabot, T. Halmos, Y. Bousquet, M. D. Bailey, S. H. Kawai, R. Coulombe, S. LaPlante, A. Jakalian, P. K. Bhardwaj, D. Wernic, P. Schroeder, M. Amad, P. Edwards, M. Garneau, J. Duan, M. Cordingley, R. Bethell, S. W. Mason, M. Bos, P. Bonneau, M. A. Poupart, A. M. Faucher, B. Simoneau, C. Fenwick, C. Yoakim and Y. Tsantrizos, *ACS Med. Chem. Lett.*, 2014, **5**, 422.
- 12 (a) R. Burikhanov, V. M. Sviripa, N. Hebbar, W. Zhang, W. J. Layton, A. Hamza, C. G. Zhan, D. S. Watt, C. Liu and V. M. Rangnekar, *Nat. Chem. Biol.*, 2014, **10**, 924; (b) V. M. Sviripa, R. Burikhanov, J. M. Obiero, Y. Yuan, J. R. Nickell, L. P. Dwoskin, C. G. Zhan, C. Liu, O. V. Tsodikov, V. M. Rangnekar and D. S. Watt, *Org. Biomol. Chem.*, 2016, **14**, 74.
- 13 M. M. Cardenas, M. A. Saputra, D. A. Gordon, A. N. Sanchez, N. Yamamoto and J. L. Gustafson, *Chem. Commun.*, 2021, **57**, 10087.
- 14 (a) K. Mori, Y. Ichikawa, M. Kobayashi, Y. Shibata, M. Yamanaka and T. Akiyama, *J. Am. Chem. Soc.*, 2013, **135**, 3964; (b) K. Mori, T. Itakura and T. Akiyama, *Angew. Chem., Int. Ed.*, 2016, **55**, 11642; (c) T. Uchikura, S. Kato, Y. Makino, M. J. Fujikawa, M. Yamanaka and T. Akiyama, *J. Am. Chem. Soc.*, 2023, **145**, 15906.
- 15 G. Liu and Y. Cao, *Adv. Synth. Catal.*, 2023, **365**, 3044.
- 16 (a) R. S. J. Proctor, H. J. Davis and R. J. Phipps, *Science*, 2018, **360**, 419; (b) J. P. Reid, R. S. J. Proctor, M. S. Sigman and R. J. Phipps, *J. Am. Chem. Soc.*, 2019, **141**, 19178; (c) K. Ermanis, A. C. Colgan, R. S. J. Proctor, B. W. Hadrys, R. J. Phipps and J. M. Goodman, *J. Am. Chem. Soc.*, 2020, **142**, 21091; (d) P. D. Bacos, A. S. K. Lahdenperä and R. J. Phipps, *Acc. Chem. Res.*, 2023, **56**, 2037.
- 17 Xiao and co-workers recently reported atroposelective synthesis of 5-arylbiopyrimidines by the combined use of chiral phosphoric acid and photocatalyst, see: D. Liang, J. R. Chen, L. P. Tan, Z. W. He and W. J. Xiao, *J. Am. Chem. Soc.*, 2022, **144**, 6040.
- 18 R. J. Phipps and B. W. Hadrys, *Synlett*, 2021, 179.
- 19 For seminal papers, see: (a) T. Akiyama, J. Itoh, K. Yokota and K. Fuchibe, *Angew. Chem., Int. Ed.*, 2004, **43**, 1566; (b) D. Uraguchi and M. Terada, *J. Am. Chem. Soc.*, 2004, **126**, 5356. For reviews, see: (c) D. Parmar, E. Sugiono, S. Raja and M. Rueping, *Chem. Rev.*, 2014, **114**, 9047; (d) D. Parmar, E. Sugiono, S. Raja and M. Rueping, *Chem. Rev.*, 2017, **117**, 10608; R. Maji, S. C. Mallojjalaa and S. E. Wheeler, *Chem. Soc. Rev.*, 2018, **47**, 1142.
- 20 For reviews, see: (a) A. Parra, S. Reboredo, A. M. M. Castro and J. Alemán, *Org. Biomol. Chem.*, 2012, **10**, 5001; (b) R. J. Phipps, G. L. Hamilton and F. D. Toste, *Nat. Chem.*, 2012, **4**, 603; (c) G.-C. Fang, Y.-F. Cheng, Z.-L. Yu, Z.-L. Li and X.-Y. Liu, *Top. Curr. Chem.*, 2019, **377**, 23.
- 21 For our study on chiral metal phosphate-catalyzed asymmetric reactions, see: (a) K. Mori, R. Isogai, Y. Kamei, M. Yamanaka and T. Akiyama, *J. Am. Chem. Soc.*, 2018, **140**, 6203; (b) I. Ibanez, M. Kaneko, Y. Kamei, R. Tsutsumi, M. Yamanaka and T. Akiyama, *ACS Catal.*, 2019, **9**, 6903.
- 22 CCDC 2286593 contains the supplementary crystallographic data of **3a**<sup>†</sup>.
- 23 The transformation of **intA** into **intB** or the following oxidation of **intB** would be the stereodetermining step of the axial chirality. Further mechanistic studies to elucidate the origin of stereochemistry are focus of ongoing investigation.

